

NASA Technical Memorandum 100215

# A Microstructural Lattice Model for Strain Oriented Problems: A Combined Monte Carlo Finite Element Technique

{NASA-TM-100215} A MICROSTRUCTURAL LATTICE MODEL FOR STRAIN ORIENTED PROBLEMS: A COMBINED MONTE CARLO FINITE ELEMENT TECHNIQUE (NASA) 32 p Avail: NTIS HC A03/MF A01 N88-10939 Unclas CSCL 11F G3/26 0106488

J. Gayda  
*Lewis Research Center*  
*Cleveland, Ohio*

and

D.J. Srolovitz  
*University of Michigan*  
*Ann Arbor, Michigan*

November 1987

**NASA**

A MICROSTRUCTURAL LATTICE MODEL FOR STRAIN ORIENTED PROBLEMS; A COMBINED  
MONTE CARLO FINITE ELEMENT TECHNIQUE

J. Gayda  
National Aeronautics and Space Administration  
Lewis Research Center  
Cleveland, Ohio 44135

and

D.J. Srolovitz  
University of Michigan  
Ann Arbor, Michigan 48109

SUMMARY

E-3824

A specialized, microstructural lattice model, termed MCFET for combined Monte Carlo Finite Element Technique, has been developed which simulates microstructural evolution in material systems where modulated phases occur and the directionality of the modulation is influenced by internal and external stresses. In this approach the microstructure is discretized onto a fine lattice. Each element in the lattice is labelled in accordance with its microstructural identity. Diffusion of material at elevated temperatures is simulated by allowing exchanges of neighboring elements if the exchange lowers the total energy of the system. A Monte Carlo approach is used to select the exchange site while the change in energy associated with stress fields is computed using a finite element technique.

The MCFET analysis has been validated by comparing this approach with a closed-form, analytical method for stress-assisted, shape changes of a single particle in an infinite matrix. Sample MCFET analyses for multiparticle problems have also been run and in general the resulting microstructural changes associated with the application of an external stress are similar to that observed in Ni-Al-Cr alloys at elevated temperatures.

INTRODUCTION

Since many of the physical properties of materials are determined by microstructure, it is important to be able to predict and control microstructural development. Recently a microstructural lattice model (refs. 1 and 2) has been developed which can in principle incorporate all relevant driving forces and kinetic considerations in a single simulation. Unlike molecular dynamics, this approach was developed specifically to predict macroscopic behavior, not atomistic behavior.

The essential elements of this approach consist of mapping the continuum microstructure onto a discrete lattice and defining interactions and dynamics for the lattice points which are analogous to those in a continuous system. Each lattice site is assigned a label which corresponds to the microstructural identity of that site. The evolution of the microstructure is governed by the appropriate dynamics and the relevant driving forces. Nonconserved dynamics

(ref. 3) applies to systems in which the internal energy is dependent on parameters which are not conserved during the temporal evolution of the system, while conserved dynamics (ref. 4) applies when said parameters are conserved. In the former instance, dynamical evolution is controlled by a Monte Carlo procedure in which a site is randomly selected and its label changed to one of the other allowed labels, if the energy of the system is lowered. In the latter instance, dynamical evolution is controlled by a Monte Carlo procedure in which a pair of neighboring sites is randomly selected and their labels exchanged if the energy of the system is lowered.

In the present paper a further refinement of the latter approach, termed MCFET for combined Monte Carlo Finite Element Technique, is developed specifically to model materials that contain modulated phases where the directionality of the modulation is strongly influenced by the application of an external stress, an example being the Ni-Al-Cr alloy system. In this approach a finite element technique is used to calculate the strain energy associated with internal and external stress fields, while microstructural evolution is controlled using a Monte Carlo procedure which employs conserved dynamics.

The first half of this paper describes the details of the MCFET approach, while the second half of the paper is devoted to sample MCFET simulations of increasing complexity.

#### MCFET APPROACH

To model microstructural changes via the MCFET approach an  $n \times n$  two-dimensional grid utilizing square elements was employed. For a realistic analysis a typical value for  $n$  could be as high as 100. The spatial identity of each element (lattice site) in the grid is uniquely defined by a global numbering scheme depicted in figure 1. Each element also has a chemical or microstructural identity which serves to define the shape, distribution, and volume fraction of all phases present in the microstructure. For a two phase microstructure each element in the grid would be associated with phase P (precipitate) or phase M (matrix) as shown in figure 1.

As previously mentioned, microstructural changes were modelled in the present analysis using an approach which is often referred to as conserved dynamics. In this approach microstructural evolution occurs by exchanges of neighboring sites and therefore the total number of elements identified with phase P and M in the aforementioned grid remain constant. The location of the exchange pair is chosen at random and the success or failure of the exchange is governed by the change in energy. An exchange which lowers the energy of the system is accepted, otherwise the exchange is rejected.

As the size of the Monte Carlo grid is finite, the external surfaces or boundaries of the grid pose a dilemma if the problem of interest is one in which bulk behavior dominates, as in the case of an "infinite" solid. To eliminate these surface effects, periodic boundary conditions were used in the present analysis. In this approach the Monte Carlo grid appears infinite, although periodic, as elements on the upper boundary are considered nearest neighbors of elements on the lower boundary while elements on the right boundary are considered nearest neighbors of elements on the left boundary.

The energy criteria, which determines the success of an exchange, will be confined to three components in the present analysis; the interfacial or surface energy, the mechanical or strain energy of an elastic solid, and the thermal energy. The interfacial energy is directly proportional to the total surface area (perimeter in this two-dimensional analysis) associated with the interface between phases P and M. The mechanical energy arises from strains generated in the solid by externally applied loads and internal misfit strains when coherent precipitate(s) are present, as in a multiphase microstructure. The calculation of the mechanical energy term for an arbitrary microstructure encountered in such an analysis is difficult if not impossible to attain via classical elasticity, however, such calculations are conceptually quite easily attained using finite element techniques, and as previously stated, will be used in the present approach. The thermal energy term,  $kT$ , is directly proportional to the temperature of the solid,  $T$ . The significance of the thermal energy is dependent on the ratio  $E/kT$ , where  $E = E_{\text{surface}} + E_{\text{strain}}$  is the change in internal energy for a given exchange. When  $E/kT \ll 0$  the probability of a successful exchange is high, but when  $E/kT \gg 0$  the probability of a successful exchange is low. If  $E/kT$  is near zero the exchange probability is near 0.5. Computationally, this is attained by accepting an exchange if  $[1 - \text{TANH}(E/kT)]/2$  is greater than a random number between 0 and 1..

Before leaving the general discussion concerning the calculation of total energy, it should be noted that scaling of these three energy components relative to one another is often the most difficult part of the problem. In many instances, experimental data for surface tension or elastic properties of individual phases are questionable or nonexistent, so one can only approximate or assume values for these physical constants. Changes in these parameters can profoundly alter the outcome of the MCFET analysis as the dominant energy term changes. This point will be examined in more detail later in this paper.

The concept of a time scale in most lattice models is related to the number of exchanges. In this paper one monte carlo time step, MCS, will be defined as  $n$  squared attempted exchanges where  $n$  is the size of the  $n \times n$  monte carlo grid.

#### FINITE ELEMENT STRESS ANALYSIS

Although finite element techniques can be applied to the present problem without great difficulty, the enormous number of exchanges to be considered in a realistic analysis would require an impractical amount of computer time to calculate the mechanical energy term over the entire monte carlo grid for every exchange. Therefore one must devise a scheme which limits the computation time per exchange. In the present analysis this is accomplished by confining the stress analysis to a small region centered about the exchange site and calculating the mechanical energy term of this smaller, local grid before and after the exchange. The value of such an approach is that while the absolute energies of the local grid may be seriously affected by limiting the area over which the stress analysis is done, the change in energy associated with the exchange is, however, less likely to be flawed, as similar errors are generated and then cancel when the difference in the pre- and post-exchange energies is calculated. Further, as the change in energy values calculated are only used to decide if a given exchange is accepted, the numerical results, and therefore the associated error, is not accumulated. The sensitivity of the error as a

function of grid size used in the stress analysis will be quantified at a later point in the paper.

The smaller, local monte carlo grid on which the stress analysis is run is shown in figure 2. It is generated from the larger, global monte carlo grid and is seen to contain 36 elements with the exchange pair residing in the 4 central elements. The actual element type used in the finite element analysis is the two-dimensional, simplex triangle, and as shown in figure 2 each monte carlo element contains two such simplex triangles. With this element type and grid size one must generate and solve a system of linear equations containing 98 unknowns for each exchange. This can be done in a fraction of a second on a mainframe computer and it is therefore possible to perform a realistic MCFET analysis which may require thousands of exchanges.

The elastic properties, modulus, Poisson's ratio, etc., of each monte carlo element are assigned values corresponding to the phase identity for that element. To model the misfit strains between precipitate and matrix, a volumetric strain is simulated by replacing the usual thermal strain term in the finite element formulation with a numerically equivalent misfit strain. For a two phase analysis in which the misfit strain is -0.1 percent, the thermal strain term of the matrix elements are set equal to 0.05 percent while the thermal strain term of the precipitate elements are set equal to -0.05 percent. Note that the thermal strain term referred to here is not related to the aforementioned thermal energy term.

The finite element code used in the present analysis is simple but nevertheless time efficient, and was adopted from the text of Segerlind (ref. 5). In this code the nodal displacements of the finite element grid are computed by minimizing the potential energy of the system for a given set of boundary conditions. From these nodal displacements one then computes the element strains and stresses, and finally the mechanical energy of the local monte carlo grid. The choice of boundary conditions are somewhat ambiguous in the present problem as one is analyzing a small section of an "infinite" solid. As previously noted, extreme accuracies of the absolute energies are not necessary in the present analysis, therefore the simplest and computational fastest boundary conditions were adopted. These set of boundary conditions eliminate rigid body motion by fixing the displacements of the central node at zero, while rigid body rotation is prevented by setting the lateral displacement of the node directly above the central node at zero. Otherwise the body is essentially unconstrained. As previously stated, the exchange pair is always contained in the four central elements of the local monte carlo grid and as a result there is no directional bias to the exchange resulting from the unconstrained or free boundary conditions used herein, this would not be true if the exchange pair were not equidistant from all the outer boundaries of the local monte carlo grid. In addition to the displacement boundary conditions, if externally applied stresses are to be modelled the appropriate loads are applied to the nodes along the outer boundaries. For a uniaxial stress state, loads of equal but opposite magnitude are applied to the upper and lower boundary nodes of the finite element grid.

The actual codes used to perform the combined monte carlo/finite element analysis maybe found in the appendix. In addition to these codes there is a complete description of the input and output data used in an analysis as well as a simplified flowchart describing the overall approach.

## INTEGRATION OF THE GRIDS

Although some description concerning integration of the finite element and monte carlo grids has preceded this point, it is felt that a separate, more detailed explanation is warranted as this process is of central importance to the present analysis. The description of this process is most readily handled by example. Given the global monte carlo grid of figure 1, one first selects a site at random and then selects one of eight adjoining elements to form the exchange pair. If these are of different identity the exchange is attempted. Taking element E[7,12] in figure 1 as the site for the exchange the next step would involve selection of a neighboring element. In the present analysis this is done by choosing a number at random between one and eight, inclusive. As seen in figure 3, this number defines the exchange pair according to the convention shown. The four central elements of the 6x6 local monte carlo grid on which the stress analysis will be done are determined by the logic described in figure 3. The remainder of the local monte carlo grid is then filled in using the information found in the global monte carlo grid. Continuing with the present example, suppose an exchange type 6 was selected, the resulting grid would appear as shown in figure 2. Note that since the exchange pair is located near the right boundary of the global monte carlo grid, figure 1, the local monte carlo grid, figure 2, is composed of elements on both the right and left hand side of the global monte carlo grid. The finite element based stress analysis is then performed on the local grid to yield the pre-exchange strain energy. This is then summed with the interfacial energy. The exchange is now performed on the local monte carlo grid and the total energy, both interfacial and strain, is recomputed for the new configuration. If the difference in the energy before and after exchange is less than the thermal energy at this position and time, the exchange is accepted and the global monte carlo grid is modified by exchanging the identity of sites E[7,12] and E[8,11] in figure 1. A new site and exchange type is chosen at random and the process is repeated. As previously stated, no numeric information concerning energy, especially strain energy, is carried forth, only the configurational changes of the global monte carlo grid affects subsequent calculations of strain and interfacial energy terms.

## VALIDATION OF THE MCFET APPROACH

Before analyzing more complex problems with multiple particle microstructures it is instructive to look at some simple one and two particle problems to understand and validate the MCFET approach. In the following analyses, thermal and surface tension effects will be ignored and the elastic properties of all phases will be taken to be isotropic.

The first and simplest example to be run tracks the path of a single precipitate, comprising one monte carlo element, over an extended period of time on a small 6x6 grid. The particle has the same elastic properties as the matrix and a misfit of -0.1 percent, further there is no applied stress. The results of this analysis are summarized in figure 4 after 100 MCS and shows the number of exchanges per site involving the single precipitate particle. Two points are to be made. First, of the approximately 3600 attempted exchanges only 200 involved the precipitate. This number is consistent with random selection of the exchange pair. Second and perhaps more important, there is no apparent positional bias introduced by the use of periodic boundaries or the finite element stress analysis.

In figure 5 a second, single element particle has been added to the 6x6 grid and after only 16 MCS the particles coalesce. Further, in this time only four exchanges involving the precipitate particles were accepted, all of which tended to diminish the separation of the two particles. This shows that there is an attractive force between these small, single element particles. This attractive force is also evident when the elastic properties of matrix and precipitate are unequal. Examining the energy change associated with these four exchanges, it is apparent that particle coalescence produces the most pronounced decrease in system energy. By comparison, the energy change of the other three exchanges was less than 10 percent of that associated with particle coalescence. The presence of this attractive force was not anticipated, as classical elasticity theory predicts misfitting particles in a matrix with identical properties are neither attracted nor repelled by one another. The origin of this force is apparently related to the finite grid size and boundary conditions employed. The discrepancy with classical elasticity does not appear to render the technique unusable, as will be shown. Rather, the most significant affect of this attraction results from the large energy decrease accompanying particle coalescence. This produces an inherent surface tension over and above that normally associated with the surface energy term routinely employed in these lattice models.

As previously stated, the size of the finite element grid must in general be smaller than the monte carlo grid for computational reasons. In this paper the size of the finite element grid will be limited to 6x6. To determine if this seriously affects the stress analysis a series of finite element analysis were run on the microstructure shown in figure 6. In these analyses, the misfit is -0.1 percent, the moduli of the particles is  $8 \times 10^9$  Pa versus  $10 \times 10^9$  Pa for the matrix, and a stress of  $3 \times 10^8$  Pa is applied. The change in strain energy for the exchange of sites P and M were then computed for a 6x6, 12x12, and 18x18 finite element grid. While the absolute energies are much different for the three grid sizes, as evident by the pre-exchange strain energy, the change in strain energies differ by less than 2 percent. Hence, it appears that the choice of a 6x6 finite element grid provides sufficient accuracy while minimizing computational requirements.

To validate the MCFET approach, microstructural shape changes of a singular particle associated with the application of a uniaxial stress field of varying magnitude and direction were examined. This problem has been analyzed by others using the approach of Eshelby. In particular, Pineau (ref. 6) has presented a thorough analysis of the single-particle problem in which the equilibrium particle shape is mapped for a variety of situations. This map has been reproduced in figure 7(a). The ratio of precipitate to matrix stiffness is plotted on the y-axis, while the ratio of applied stress to misfit, normalized by the matrix stiffness, is plotted on the x-axis. As seen figure 7(a), the application of stress can have three effects; the particle may remain spherical, the particle may elongate such that the elongated direction is parallel to the stress axis, or the particle may elongate such that elongated direction is perpendicular to the stress axis. Also shown on this map are discrete symbols representing MCFET runs. In these instances the starting microstructures consisted of a single, square particle, containing four elements, as shown in figure 7(b). The finite element grid was 6x6 while the monte carlo grid was 12x12, thereby assuring that the particle would be essentially contained in an infinite matrix. The final particle shape which evolved was a singular, rectangular particle, 4x1, with one exception. This particle

remained square. These shapes were analogous to that predicted by the Eshelby approach. The agreement between the two techniques shows the additional interelement attraction documented in figure 5 did not seriously influence the outcome of the MCFET analysis of the single particle problem.

At this time it is instructive to extend this analysis to the two multi-element, particle problem pictured in figure 8. Here one examines the effect of interparticle separation,  $R_p$ , on particle shape as a function of applied stress. This analysis will be limited to a precipitate moduli and misfit of  $8 \times 10^9$  Pa and  $-0.1$  percent respectively, and a matrix moduli of  $10 \times 10^9$  Pa. Such a choice traverses the Pineau map, figure 7(a), at  $E_p/E_m$  of 0.8. It is apparent that the interparticle separation influences the stress level at which the initial configuration becomes unstable. The configuration which evolves is still in general agreement with Pineau's map for the single particle problem. While one might suspect adjacent particles to have some effect, it is unclear at this point how much of said effect is an artifact of the finite element technique similar to that associated with the interelement attraction documented in figure 5, and how much is a "real" effect that should be modelled.

### SCALING EFFECTS

To this point the MCFET analyses have been run without temperature or surface tension effects. The exchange criteria has been based solely on the change in strain energy. As a consequence the absolute dimensions of a particle are irrelevant. However, when surface tension effects are included, assigning an absolute dimension to a particle is very important as surface energy effects scale with the square of the particle size (surface area) while strain energy effects scale with the cube of the particle size (volume). In the remaining MCFET analyses the effects of surface tension and temperature will be included. As a starting point a surface tension of  $2 \times 10^{-2}$  J/m<sup>2</sup> will be assumed, and each monte carlo element will be assigned a length unit of  $1 \times 10^{-6}$  m on edge. This length scale is appropriate for microstructural analysis.

To introduce temperature effects in the problem, the thermal energy term,  $kT$ , is included in the energy balance, as described in the section entitled MCFET APPROACH. In essence the magnitude of  $kT$  is compared to other energy terms. In the present analysis,  $k$  is equated to the surface tension. The rationale for this approach is, it balances the thermal and surface energy terms of an exchange which creates a single interface between precipitate and matrix when  $T = 1$ . In other words, the solution temperature of the precipitate is near unity in the absence of strain effects. To demonstrate this, simulations were run with  $kT$  equal to  $1 \times 10^{-2}$ ,  $2 \times 10^{-2}$ , and  $3 \times 10^{-2}$  ( $T = 0.5, 1.0, \text{ and } 1.5$ ). In each case the starting microstructure was a single, square particle, comprising four elements on a  $12 \times 12$  monte carlo grid. The misfit was taken to be  $-0.1$  percent, the precipitate moduli was  $8 \times 10^9$  Pa versus  $10 \times 10^9$  Pa for the matrix, and there was no externally applied stress. As seen in figure 9, at a temperature corresponding to  $kT = 1 \times 10^{-2}$  the particle did not break up nor did it change shape. At  $kT = 3 \times 10^{-2}$  the four element particle broke up into four single, element particles after 7 MCS. This temperature is obviously at or above the solution temperature of the precipitate for the given parameters. At  $kT = 2 \times 10^{-2}$  the particle breaks up briefly at 8 MCS but rapidly coalesces. However, as shown in figure 9, the aspect ratio is continually changing as there is a considerable amount of surface mobility at this temperature.



As previously stated the choice of a length scale can affect the surface area to volume ratio, and therefore the relative magnitude of the various energy terms. To illustrate this effect on microstructural evolution the preceding problem was rerun using a value of  $kT = 2e-2$  and three length scales;  $1e-5$ ,  $1e-6$ , and  $1e-7$  m, all of which are still physically reasonable choices. As seen in figure 10, on decreasing the length scale to  $1e-7$  m the particle becomes more prone to break up due to increased mobility of the constituent elements. On increasing the length scale to  $1e-5$  m, the particle is seen to be stable out to 16 MCS. Further, even surface mobility has been eliminated as surface tension effects completely overwhelm thermal and strain energy effects. This example points out the importance of choosing an appropriate length scale and surface tension number for the problem at hand as such choices can profoundly alter the relative importance of each energy term.

### STRESS ASSISTED MICROSTRUCTURAL EVOLUTION

In the preceding sections various aspects of the MCFET approach have been examined and validated to some degree. In this section, the effects of an applied stress on a single and multiple particle problem will be examined under more realistic conditions, surface tension and thermal effects will be included. Each of these analyses will be run with a  $12 \times 12$  monte carlo grid initially containing  $2 \times 2$  square particle(s) with a misfit of  $-0.1$  percent. A matrix moduli of  $10e10$  Pa and a precipitate moduli of  $8e10$  Pa will be assumed. Further, a surface tension value of  $2e-2$  J/m<sup>2</sup> and  $kT$  of  $2e-2$  will be used with the length scale set at  $1e-6$  m per element.

The effect of a tensile and compressive stress on a single square particle will be examined first. These results are presented in figure 11 along with that for an unstressed particle. In this figure the overall aspect ratio,  $A_r$ , being the averaged height to width ratio of all particles is plotted as a function of simulated time. This definition was adopted as it is possible for the particle to break up. With no applied stress the aspect ratio flip flops about unity and it appears that a single particle is the most stable configuration as it breaks up only briefly at 8 MCS. Under a tensile stress of  $3e8$  Pa, the aspect ratio climbs above unity near 6 MCS and remains there but for a brief time at 8 MCS. At about 12 MCS the particle breaks up but the aspect ratio still remains above unity. When a compressive stress of  $-3e8$  Pa is applied, the particle first breaks up near 4 MCS and shortly thereafter the aspect ratio falls below unity where it remains even when the particles coalesce between 6 and 7 MCS. Although the kinetics of the shape evolution and particle stability are different from that obtained when surface and thermal effects are absent, figure 7(a), the aspect ratios obtained here for tension and compression are in general agreement with the final equilibrium shapes shown in figure 7(a).

The effect of applied stress on a multiparticle microstructure is examined next. The initial microstructure, containing approximately 45 vol % of precipitate arranged as a regular array of square particles, is illustrated in figure 12. Also shown are the resulting microstructures after 12 MCS when an applied stress of  $3e8$  or  $-3e8$  Pa is present. As seen here, the compressive stress produces a microstructure in which alternate layers of precipitate and matrix are aligned perpendicular to the stress axis. When the applied stress is tensile, a less regular microstructure evolves in which the alignment of alternating layers of precipitate and matrix is parallel to the stress axis.

The less regular nature of the microstructure under tension was apparent very early in the analysis. That this should occur is not totally surprising as the Pineaup map shows this type of structure, N region in figure 7(a), is stable over a rather limited area. The continuous, layered microstructure which evolved in the simulations is similar to that observed in real systems, such as the Ni-Al-Cr alloys. In these alloys the microstructure, prior to the application of an external stress, consists of a regular array of  $\gamma'$  precipitates in a continuous  $\gamma$  matrix, much like the idealized, starting microstructure shown in figure 12. On applying an external stress at elevated temperatures near 1000C, these alloys form continuous layers of the  $\gamma$  and  $\gamma'$  phases. This morphology is often referred to as a rafted microstructure. For tensile loads, raft formation perpendicular to the stress axis have been observed for some alloy compositions (ref. 7), while still other alloy compositions form rafts which are parallel to the stress axis (ref. 8). The behavior of a particular alloy is believed to be dependent on the misfit and elastic properties of precipitate and matrix. On applying a compressive load, the sense of the rafting orientation has been observed to reverse, as was the case for the MCFET simulation.

### SUMMARY OF RESULTS

A specialized, microstructural lattice model, MCFET, has been developed which simulates microstructural evolution in material systems where modulated phases occur and directionality of the modulation is influenced by internal and external stresses. The energy of the stress fields is estimated with a finite element technique while microstructural evolution is simulated with a Monte Carlo approach in which conserved dynamics is used.

The MCFET analysis has been validated by comparing this approach with a closed-form, analytical method for the single-particle, infinite matrix problem. Sample MCFET analyses for a multiparticle problem have also been run and in general the resulting microstructures are similar to those observed in the Ni-Al-Cr alloy system.

Although the MCFET approach appears to be a promising analytical tool as is, much more development is possible. Some areas for future work include:

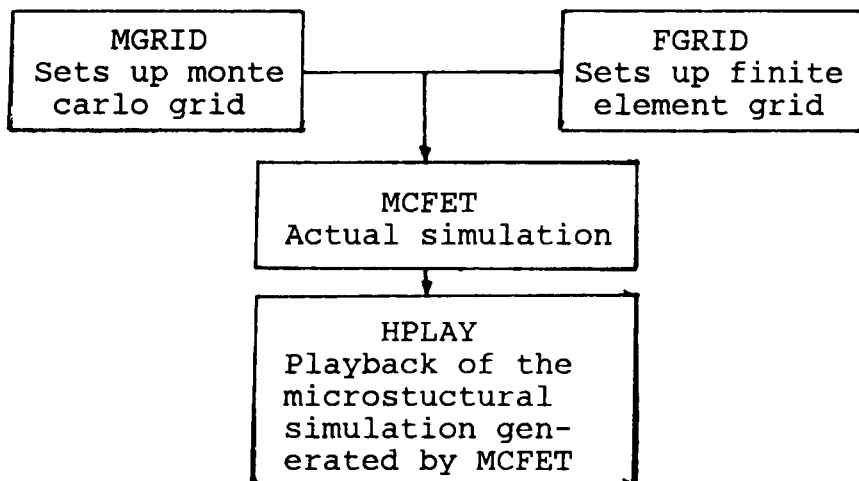
1. Improving the accuracy of the finite element stress analysis by developing more accurate boundary conditions, use of complex grid elements, and development of a variable grid geometry to more accurately represent the distant continuum.
2. Employing three dimensional analysis as opposed to the current two-dimensional analysis.
3. Develop a dislocation simulator, as misfit dislocations are very important to this class of problem.

### ACKNOWLEDGEMENT

The authors would like to thank R.A. MacKay and A.D. Freed of NASA Lewis Research Center for helpful discussions on Ni-Al-Cr alloy behavior and elasticity theory respectively.

## APPENDIX

The MCFET analysis comprises four computer programs, MGRID, FGRID, MCFET and HPLAY. Printouts of each code may be found at the end of this appendix. Each of these codes is written in FORTRAN77 and can be run on an IBM 370 class, mainframe computer. A flowchart shown below describes how these codes work together in a MCFET analysis:



As indicated above MGRID and FGRID are run first. The inputs to MGRID are:

- 1)Size of the  $n \times n$  monte carlo grid [MGR0090]
- 2)Location of particle [MGR0120]
- 3)Size of particle [MGR0150]

The information in brackets refers to the line number of the appropriate statements in MGRID. MGRID continues to ask for the location and size of additional particles until the user responds with 0,0 as input to [MGR0120]. The output of MGRID is a file (FILEDEF 10) to be used as input by MCFET. FGRID has a singular input:

- 1)Size of the  $n \times n$  finite element grid [FGR0050]

and also produces a file (FILEDEF 11) to be used as input by MCFET. In this paper the value of  $n$  in FGRID is generally set at 6.

MCFET is run next and has the following inputs:

- 1)Unit length of monte carlo element [MCF0270]
- 2)Temperature [MCF0290]
- 3)Surface tension [MCF0310]
- 4)Random number seed and number of finite element calculations [MCF0330]
- 5)Applied stress, misfit parameter, and size of monte carlo grid [MCF0350]
- 6)Elastic parameters of matrix  $D_1, D_2, D_3$  [MCF0370]
- 7)Elastic parameters of precipitate particles  $D_1, D_2, D_3$  [MCF0390]

Most of the above have been discussed in the body of this paper, however, some explanation is in order. First, the dimensions of all inputs must be consistent. Second, the random number seed [MCF0330] is used by the random number generator GGUBS, which is a predefined IMSL function; the number of finite element calculations [MCF0330] is used to limit the computer time per run; and the misfit parameter [MCF0350] is equal to  $-d/2$  where  $d$  is the alloy misfit. Finally, the elastic parameters are defined as follows:

D1=Elastic modulus  
D2=0.3\*D1  
D3=0.4\*D1

for the analysis employed here.

After MCFET completes the specified number of finite element calculations the resulting microstructure is displayed and the code then requests the following additional inputs:

- 1)Change the number of finite element calculations [MCF3500]
- 2)Number of finite element calculations [MCF3600]

If one responds with 0 to [MCF3500] the run is terminated, otherwise MCFET requests input to [MCF3600] and the process is repeated until a response of 0 is provided as input to [MCF3500]. On termination all information concerning microstructural evolution is contained in two files (FILEDEF 12 and 13).

As indicated in the flowchart HPLAY is then run to view microstructural evolution. The inputs to HPLAY are a file produced by MCFET (FILEDEF 12) and the following:

- 1)Number of finite element calculations and size of the monte [HPL0050]  
carlo grid

The first item is equal to the last value of said parameter used in MCFET.

```

C   MONTE CARLO GRID (MGRID)
    INTEGER MGRID(25,25)
    INTEGER R,C
    DO 10 R=1,25
    DO 10 C=1,25
    MGRID(R,C)=1
10  CONTINUE
    PRINT *, 'SIZE OF MONTE CARLO GRID'
    READ *,NGS [MGR0090]
    PRINT *, 'ORIGIN TAKEN AS LOWER LEFT CORNER'
20  PRINT *, 'ROW, COLUMN OF PARTICLE ORIGIN' [MGR0120]
    READ *,R,C
    IF (R .EQ. 0) GO TO 35
    PRINT *, 'PARTICLE HEIGHT, WIDTH'
    READ *,H,W [MGR0150]
    DO 30 I=R,R+H-1
    DO 30 J=C,C+W-1
    MGRID(I,J)=2
30  CONTINUE
    GO TO 20
35  CONTINUE
    DO 40 I=1,NGS
    DO 40 J=1,NGS
    WRITE (10,50) I,J,MGRID(I,J)
50  FORMAT (3I4)
40  CONTINUE
    DO 70 R=NGS,1,-1
    WRITE (6,100) (MGRID(R,C),C=1,NGS)
70  CONTINUE
100 FORMAT (24I3)
    STOP
    END

```

C

```

GRID GENERATION CODE (FGRID)
INTEGER N1(1250),N2(1250),N3(1250),P(12),Q(12),NS(6,1250),LS
REAL B(3,6,1250),AR2(1250)
PRINT *, ' INPUT LATTICE SIZE AS N X N'
READ *, LS
[ FGR0050]
NE=(2*LS)*LS
NP=(LS+1)**2
NC=LS
NR=2*LS
N4=INT(NP**0.5)
N5=2*N4
P(1)=1
P(2)=2
P(3)=N4+1
P(4)=2
P(5)=N4+2
P(6)=N4+1
P(7)=2
P(8)=N4+3
P(9)=N4+2
P(10)=2
P(11)=3
P(12)=N4+3
Q(1)=N4+1
Q(2)=N5+2
Q(3)=N5+1
Q(4)=N4+1
Q(5)=N4+2
Q(6)=N5+2
Q(7)=N4+2
Q(8)=N4+3
Q(9)=N5+2
Q(10)=N4+3
Q(11)=N5+3
Q(12)=N5+2
ITERM1=NC/2
ITERM2=NR/4
DO 3 I=1, ITERM1
DO 3 J=1, ITERM2
DO 3 K=1, 4
I1=K+4*(J-1)+2*NR*(I-1)
I2=3*(K-1)
I3=2*(I-1)*INT(NP**0.5)+2*(J-1)
IDUM1=1+I2
IDUM2=2+I2
IDUM3=3+I2
N1(I1)=P(IDUM1)+I3
N2(I1)=P(IDUM2)+I3
N3(I1)=P(IDUM3)+I3
I1=K+4*(J-1)+(2*(I-1)+1)*NR
N1(I1)=Q(IDUM1)+I3
N2(I1)=Q(IDUM2)+I3
N3(I1)=Q(IDUM3)+I3
CONTINUE

```

3

```

DO 4 I=1,NE
IY1=(N1(I)-1)/(LS+1)
X1=(N1(I)-IY1*(LS+1))-1
IY2=(N2(I)-1)/(LS+1)
X2=(N2(I)-IY2*(LS+1))-1
IY3=(N3(I)-1)/(LS+1)
X3=(N3(I)-IY3*(LS+1))-1
Y1=IY1
Y2=IY2
Y3=IY3
B(1,1,I)=Y2-Y3
B(1,3,I)=Y3-Y1
B(1,5,I)=Y1-Y2
B(2,2,I)=X3-X2
B(2,4,I)=X1-X3
B(2,6,I)=X2-X1
B(3,1,I)=B(2,2,I)
B(3,2,I)=B(1,1,I)
B(3,3,I)=B(2,4,I)
B(3,4,I)=B(1,3,I)
B(3,5,I)=B(2,6,I)
B(3,6,I)=B(1,5,I)
AR2(I)=X2*Y3+X3*Y1+X1*Y2-X2*Y1-X3*Y2-X1*Y3
NS(1,I)=N1(I)*2-1
NS(2,I)=N1(I)*2
NS(3,I)=N2(I)*2-1
NS(4,I)=N2(I)*2
NS(5,I)=N3(I)*2-1
NS(6,I)=N3(I)*2
WRITE (11,6) I,AR2(I)
WRITE (11,7) NS(1,I),NS(2,I),NS(3,I),NS(4,I),NS(5,I),NS(6,I)
DO 9 J=1,3
DO 9 K=1,6
WRITE (11,8) B(J,K,I)
6   FORMAT (I4,F10.4)
7   FORMAT (6I4)
8   FORMAT (E12.6)
9   CONTINUE
4   CONTINUE
STOP
END

```

```

C   COMBINED MONTE CARLO FINITE ELEMENT STRESS ANALYSIS (MCFET)
C   THIS VERSION OF THE CODE INCLUDES RANDOM THERMAL EFFECTS
C   THIS VERSION ALSO INCLUDES SURFACE ENERGY EFFECTS
C   MAXIMUM SIZE OF MONTE CARLO GRID 25X25 (MGRID DATA)
C   STRESS ANALYSIS DONE ON A 6X6 FINITE ELEMENT GRID (FGRID DATA)
C     98 GLOBAL DEGREES OF FREEDOM (NP)
C     72 TRIANGULAR SIMPLEX ELEMENTS (NE)
C     BANDWIDTH=18 (NBW)
C
C   INPUT DATA
C
C   DOUBLE PRECISION DSEED
C   INTEGER R,C,RO,CO,R1,C1,RN,CN,RS,CS,E
C   INTEGER M(6,6),MGRID(25,25),NPHAS(72),NS(6,72)
C   REAL GF(98),GU(98),GSM(98,98),AR2(72),RN3(3)
C   REAL B(3,6,72),D(3,3,2),CM(6,3),ESM(6,6),EF(6),STRA(3),STRE(3)
C   TIM=0.0
C   T=1.0
C   NP=98
C   NE=72
C   NBW=18
C   NMCS=0
C   CALL ERRSET (207,0,-1)
C   CALL ERRSET (208,0,-1)
C   CALL ERRSET (209,0,-1)
C   PRINT *, 'UNIT LENGTH'
C   READ *,UL [MCF0270]
C   PRINT *, 'TEMPERATURE (0=COLD TO 1=HOT)'
C   READ *,TEMP [MCF0290]
C   PRINT *, 'SURFACE ENERGY OF INTERFACE'
C   READ *,SURFE [MCF0310]
C   PRINT *, 'DSEED, ITERATIONS'
C   READ *,DSEED,ITER [MCF0330]
C   PRINT *, ' YLOAD, EPHAS1, SIZE OF MONTE CARLO GRID'
C   READ *,YLOAD,EPHAS1,NLS [MCF0350]
C   PRINT *, 'D1, D2, D3 FOR PHASE 1'
C   READ *,D1P1,D2P1,D3P1 [MCF0370]
C   PRINT *, 'D1, D2, D3 FOR PHASE 2'
C   READ *,D1P2,D2P2,D3P2 [MCF0390]
C   EPHAS2=-EPHAS1
C   WRITE (12,62) YLOAD,DSEED
C   WRITE (12,63) D1P1,D2P1,D3P1,EPHAS1
C   WRITE (12,63) D1P2,D2P2,D3P2,EPHAS2
C   WRITE (12,64) TEMP,SURFE,UL
62  FORMAT (2E12.6)
63  FORMAT (3E12.6,E12.6)
64  FORMAT (3E12.6)
C   YLOAD=YLOAD*UL
C   INPUT MGRID DATA
C   DO 10 R=1,NLS
C   DO 10 C=1,NLS
C   READ (10,15) IDUM,JDUM,MGRID(R,C)
C   WRITE (12,15) IDUM,JDUM,MGRID(R,C)
15  FORMAT (3I4)

```



```

10 CONTINUE
C INPUT FGRID DATA
DO 20 I=1,NE
READ (11,25) IDUM,AR2(1)
READ (11,35) NS(1,I),NS(2,I),NS(3,I),NS(4,I),NS(5,I),NS(6,I)
DO 30 J=1,3
DO 30 K=1,6
READ (11,45) B(J,K,I)
25 FORMAT (I4,F10.4)
35 FORMAT (6I4)
45 FORMAT (E12.6)
30 CONTINUE
20 CONTINUE
C CONSTRUCT MATERIALS PROPERTY MATRIX
D(1,1,1)=D1P1*UL
D(2,2,1)=D1P1*UL
D(3,3,1)=D3P1*UL
D(1,2,1)=D2P1*UL
D(2,1,1)=D2P1*UL
D(1,3,1)=0.0
D(3,1,1)=0.0
D(2,3,1)=0.0
D(3,2,1)=0.0
D(1,1,2)=D1P2*UL
D(2,2,2)=D1P2*UL
D(3,3,2)=D3P2*UL
D(1,2,2)=D2P2*UL
D(2,1,2)=D2P2*UL
D(1,3,2)=0.0
D(3,1,2)=0.0
D(2,3,2)=0.0
D(3,2,2)=0.0
C
C MAIN CONTROL LOOP
C
C SITE AND EXCHANGE SELECTION
11 IF (NMCS .GE. ITER) GO TO 21
CALL GGUBS(DSEED,3,RN3)
RO=INT(RN3(1)*NLS+1)
CO=INT(RN3(2)*NLS+1)
E=INT(RN3(3)*8+1)
TIM=TIM+1
R1=RO
C1=CO
IF (E .EQ. 1 .OR. E .EQ. 5 .OR. E .EQ. 8) C1=C0+1
IF (E .EQ. 6 .OR. E .EQ. 3 .OR. E .EQ. 7) C1=C0-1
IF (E .EQ. 6 .OR. E .EQ. 2 .OR. E .EQ. 5) R1=R0+1
IF (E .EQ. 7 .OR. E .EQ. 4 .OR. E .EQ. 8) R1=R0-1
IF (R1 .GT. NLS) R1=R1-NLS
IF (R1 .LT. 1) R1=R1+NLS
IF (C1 .GT. NLS) C1=C1-NLS
IF (C1 .LT. 1) C1=C1+NLS
IF (MGRID(RO,CO) .EQ. MGRID(R1,C1)) GO TO 11

```

```

NMCS=NMCS+1
C   CONSTRUCT M ARRAY BEFORE EXCHANGE
    IF (E .EQ. 1 .OR. E .EQ. 5) THEN
        RS=3-R0
        CS=3-C0
    END IF
    IF (E .EQ. 2 .OR. E .EQ. 6) THEN
        RS=3-R0
        CS=4-C0
    END IF
    IF (E .EQ. 3 .OR. E .EQ. 7) THEN
        RS=4-R0
        CS=4-C0
    END IF
    IF (E .EQ. 4 .OR. E .EQ. 8) THEN
        RS=4-R0
        CS=3-C0
    END IF
    DO 40 R=6,1,-1
    DO 40 C=1,6
    RN=R-RS
    CN=C-CS
    IF (RN .GT. NLS) RN=RN-NLS
    IF (RN .LT. 1) RN=RN+NLS
    IF (CN .GT. NLS) CN=CN-NLS
    IF (CN .LT. 1) CN=CN+NLS
    M(R,C)=MGRID(RN,CN)
40  CONTINUE
    DO 50 R=1,6
    DO 50 C=1,6
    IDUM=6*R+C-6
    NPHAS(2*IDUM)=M(R,C)
    NPHAS(2*IDUM-1)=M(R,C)
50  CONTINUE
C   SURFACE AREA BEFORE EXCHANGE
    SURFO=0
    DO 59 I=3,4
    DO 59 J=2,4
    IF (M(I,J) .EQ. M(I,J+1)) SURFO=SURFO+1
    IF (M(J,I) .EQ. M(J+1,I)) SURFO=SURFO+1
59  CONTINUE
    SURFO=12-SURFO
    PATH=1
    TMSE=0.0
    GO TO 31
C   CONSTRUCT M ARRAY AFTER EXCHANGE
41  TMSEO=TMSE
    PATH=2
    TMSE=0.0
    IF (E .EQ. 1) THEN
        MO=M(3,3)
        M(3,3)=M(3,4)
        M(3,4)=MO
    END IF

```

```

IF (E .EQ. 2) THEN
  MO=M(3,4)
  M(3,4)=M(4,4)
  M(4,4)=MO
END IF
IF (E .EQ. 3) THEN
  MO=M(4,4)
  M(4,4)=M(4,3)
  M(4,3)=MO
END IF
IF (E .EQ. 4) THEN
  MO=M(4,3)
  M(4,3)=M(3,3)
  M(3,3)=MO
END IF
IF (E .EQ. 5 .OR. E .EQ. 7) THEN
  MO=M(3,3)
  M(3,3)=M(4,4)
  M(4,4)=MO
END IF
IF (E .EQ. 6 .OR. E .EQ. 8) THEN
  MO=M(3,4)
  M(3,4)=M(4,3)
  M(4,3)=MO
END IF
DO 60 R=1,6
DO 60 C=1,6
IDUM=6*R+C-6
NPHAS(2*IDUM)=M(R,C)
NPHAS(2*IDUM-1)=M(R,C)
60 CONTINUE
C SURFACE AREA AFTER EXCHANGE
SURFN=0
DO 69 I=3,4
DO 69 J=2,4
IF (M(I,J) .EQ. M(I,J+1)) SURFN=SURFN+1
IF (M(J,I) .EQ. M(J+1,I)) SURFN=SURFN+1
69 CONTINUE
SURFN=12-SURFN
GO TO 31
C COMPARE ENERGY BEFORE AND AFTER EXCHANGE
51 TMSSEN=TMSE
ECHANG=TMSSEN-TMSEO+(SURFN-SURFO)*SURFE
NEX=0
PROBKT=0.5*(1.0-TANH(ECHANG/(2.0*TEMP)))
CALL GGUBS(DSEED,1,RN3)
IF (RN3(1) .LE. PROBKT) THEN
  NEX=1
  MO=MGRID(R0,C0)
  MGRID(R0,C0)=MGRID(R1,C1)
  MGRID(R1,C1)=MO
END IF
65 WRITE (12,65) NMCS,R0,C0,R1,C1,NEX,ECHANG,TIM
FORMAT (I6,5I4,2E12.6)

```

```

      GO TO 11
C
C   MECHANICAL ENERGY CALCULATION
C
C   CONSTRUCT STIFFNESS MATRIX AND FORCE MATRIX
31  DO 70 I=1,NP
      DO 80 J=1,NP
      GSM(I,J)=0.0
80  CONTINUE
      GF(I)=0.0
70  CONTINUE
      DO 90 KK=1,NE
      IF (NPHAS(KK) .EQ. 1) THEN
          ET=EPHAS1
      ELSE
          ET=EPHAS2
      END IF
C   CALCULATE CM=BT X D
      DO 100 I=1,6
      DO 100 J=1,3
      CM(I,J)=0.0
      DO 100 K=1,3
      CM(I,J)=CM(I,J)+B(K,I,KK)*D(K,J,NPHAS(KK))
100  CONTINUE
C   MATRIX MULTIPLICATION TO OBTAIN ESM AND EF
      DO 110 I=1,6
      SUM1=0.0
      DO 120 K=1,2
      SUM1=SUM1+CM(I,K)*ET
120  CONTINUE
      DO 110 J=1,6
      SUM=0.0
      DO 130 K=1,3
      SUM=SUM+CM(I,K)*B(K,J,KK)
130  CONTINUE
      ESM(I,J)=SUM*T/(2.0*AR2(KK))
      EF(I)=SUM1*T/2.0
110  CONTINUE
C   INSERT ELEMENT MATRIX INTO GLOBAL MATRIX
      DO 140 I=1,6
      II=NS(I,KK)
      GF(II)=GF(II)+EF(I)
      DO 140 J=1,6
      JJ=NS(J,KK)
      GSM(II,JJ)=GSM(II,JJ)+ESM(I,J)
140  CONTINUE
90  CONTINUE
C   ENFORCE BOUNDARY CONDITIONS
      DO 260 I=49,51
      IB=I
      IF (I .EQ. 51) IB=63
      BV=0.0
      GSMO=GSM(IB,IB)
      DO 270 J=1,NP

```

```

      GSM(IB,J)=0.0
      GSM(J,IB)=0.0
270  CONTINUE
      GF(IB)=0.0
      GSM(IB,IB)=GSMO
260  CONTINUE
C    APPLY BOUNDARY LOADS
      DO 150 I=1,7
      IYL=2*I
      IYU=2*(42+I)
      GF(IYL)=GF(IYL)-YLOAD
      GF(IYU)=GF(IYU)+YLOAD
150  CONTINUE
C    TRIANGULARIZE SYSTEM OF LINEAR EQUATIONS
      DO 160 N=1,NP-1
      NFIN=N+NBW-1
      IF (NFIN .GT. NP) NFIN=NP
      DO 170 I=N+1,NFIN
      RM=GSM(I,N)/GSM(N,N)
      DO 180 J=N+1,NFIN
      GSM(I,J)=GSM(I,J)-GSM(N,J)*RM
180  CONTINUE
      GF(I)=GF(I)-GF(N)*RM
170  CONTINUE
160  CONTINUE
C    SOLVE LINEAR SYSTEM OF EQUATIONS BY BACKWARD SUBSTITUION
      GU(NP)=GF(NP)/GSM(NP,NP)
      DO 190 I=NP-1,1,-1
      SUM=0.0
      NFIN=I+NBW-1
      IF (NFIN .GT. NP) NFIN=NP
      DO 200 J=I+1,NFIN
      SUM=SUM+GSM(I,J)*GU(J)
200  CONTINUE
      GU(I)=(GF(I)-SUM)/GSM(I,I)
190  CONTINUE
C    CALCULATE STRESS AND STRAIN
      DO 210 N=1,NE
      DO 220 I=1,3
      STRA(I)=0.0
      DO 220 K=1,6
      STRA(I)=STRA(I)+B(I,K,N)*GU(NS(K,N))/AR2(N)
220  CONTINUE
      DO 230 I=1,3
      IF (NPHAS(N) .EQ. 1) THEN
        ET=EPHAS1
      ELSE
        ET=EPHAS2
      END IF
      IF (I .EQ. 3) ET=0.0
      STRE(I)=0.0
      DO 230 K=1,3

```

```

        STRE(I)=STRE(I)+D(I,K,NPHAS(N))*(STRA(K)-ET)
230    CONTINUE
C      CALCULATE STRAIN ENERGY
        STE=0.0
        DO 240 I=1,3
        IF (NPHAS(N) .EQ. 1) THEN
            ET=EPHAS1
        ELSE
            ET=EPHAS2
        END IF
        IF (I .EQ. 3) ET=0.0
        STE=STE+STRE(I)*(STRA(I)-ET)
240    CONTINUE
        TMSE=TMSE+STE*AR2(N)
210    CONTINUE
C      CALCULATE POTENTIAL ENERGY OF APPLIED LOADS
        SUMPU=0.0
        DO 250 I=1,7
        IYL=2*I
        IYU=2*(42+I)
        SUMPU=SUMPU+YLOAD*(GU(IYU)-GU(IYL))
250    CONTINUE
C      CALCULATE TOTAL MECHANICAL ENERGY AND RETURN TO CONTROL LOOP
        TMSE=TMSE/4-SUMPU
        IF (PATH .EQ. 1) GO TO 41
        IF (PATH .EQ. 2) GO TO 51
C      OUTPUT FINAL GRID TO SCREEN AND FILE
21    PRINT *, 'CHANGE ITER (1=YES 0=NO)'
        READ *, IDUM1
        PRINT *, 'GRID @ NMCS=', NMCS
        PRINT *, 'TIME=', TIM/(NLS*NLS)
        DO 280 R=NLS,1,-1
        WRITE (6,55) (MGRID(R,C),C=1,NLS)
55    FORMAT (24I3)
280    CONTINUE
        IF (IDUM1 .EQ. 0) GO TO 520
        PRINT *, 'ITER=', ITER
        PRINT *, 'NEW VALUE FOR ITER'
        READ *, ITER
        GO TO 11
        [MCF3500]
520    DO 500 I=1,NLS
        DO 500 J=1,NLS
        WRITE (13,510) I,J,MGRID(I,J)
510    FORMAT (3I4)
500    CONTINUE
        STOP
        END

```

[MCF3500]

[MCF3600]

```

C    PLAYBACK
    INTEGER MGRID(25,25)
    INTEGER R,C,RO,CO,R1,C1
    PRINT *, 'ITERATIONS, SIZE OF GRID'
    READ *, ITER,NGS
    READ (12,62) YLOAD,DSEED
    WRITE (6,62) DSEED,YLOAD
62   FORMAT (2E12.6)
    READ (12,63) D1P1,D2P1,D3P1,EPHAS1
    WRITE (6,63) D1P1,D2P1,D3P1,EPHAS1
    READ (12,63) D1P2,D2P2,D3P2,EPHAS2
    WRITE (6,63) D1P2,D2P2,D3P2,EPHAS2
63   FORMAT (3E12.6,E12.6)
    READ (12,64) TEMP,SURFE,UL
    WRITE (6,64) TEMP,SURFE,UL
64   FORMAT (3E12.6)
    DO 10 R=1,NGS
    DO 10 C=1,NGS
    READ (12,20) IDUM,JDUM,MGRID(R,C)
20   FORMAT (3I4)
10   CONTINUE
    DO 30 R=NGS,1,-1
    WRITE (6,40) (MGRID(R,C),C=1,NGS)
40   FORMAT (24I3)
30   CONTINUE
70   READ (12,60) NMCS,RO,CO,R1,C1,NEX,ECHANG,TIM
60   FORMAT (I6,5I4,2E12.6)
    IF (NEX .EQ. 0) GO TO 130
    MO=MGRID(RO,CO)
    MGRID(RO,CO)=MGRID(R1,C1)
    MGRID(R1,C1)=MO
    PRINT *, 'NMCS=',NMCS,'E CHANGE=',ECHANG,'TIME=',TIM
    DO 100 R=NGS,1,-1
    WRITE (6,110) (MGRID(R,C),C=1,NGS)
110  FORMAT (24I3)
100  CONTINUE
130  IF (NMCS .GE. ITER) GO TO 120
    IF (NEX .EQ. 0) GO TO 70
    GO TO 70
120  STOP
    END

```

[HPL0050]

## REFERENCES

1. Anderson, M.P., et al.: Computer Simulation of Grain Growth - I. Kinetics. Acta Met. vol. 32, no. 5, May 1984, pp. 783-791.
2. Srolovitz, D.J., et al.: Computer Simulation of Grain Growth - II. Grain Size Distribution. Acta Met. vol. 32, no. 5, May 1984, pp. 793-802.
3. Glauber, R.J.: Time-Dependent Statistics of the Ising Model. J. Math. Phys., vol. 4, no. 2, Feb. 1963, pp. 294-322.
4. Kawasaki, K.: Kinetics of Ising Models. Phase Transitions in Critical Phenomena, Vol. 2, C. Domb and M.S. Green, eds., Academic Press, 1972, pp. 443-501.
5. Segerlind, L.J.: Applied Finite Element Analysis, Wiley, New York, 1976.
6. Pineau, A.: Influence of Uniaxial Stress on the Morphology of Coherent Precipitates During Coarsening - Elastic Energy Considerations. Acta Met., vol. 24, no. 6, June 1976, pp. 559-564.
7. MacKay, R.A.; and Ebert, L.J.: The Development of  $\gamma$ - $\gamma'$  Lamellar Structures in a Nickel-Base Superalloy During Elevated Temperature Mechanical Testing. Metall. Trans. A, vol. 16, no. 11, Nov. 1985, pp. 1969-1982.
8. Carry, C.; and Strudel, J.L.: Apparent and Effective Creep Parameters in Single Crystals of a Nickel Base Superalloy - II. Secondary Creep. Acta Met., vol. 26, no. 5, May 1978, pp. 859-870.



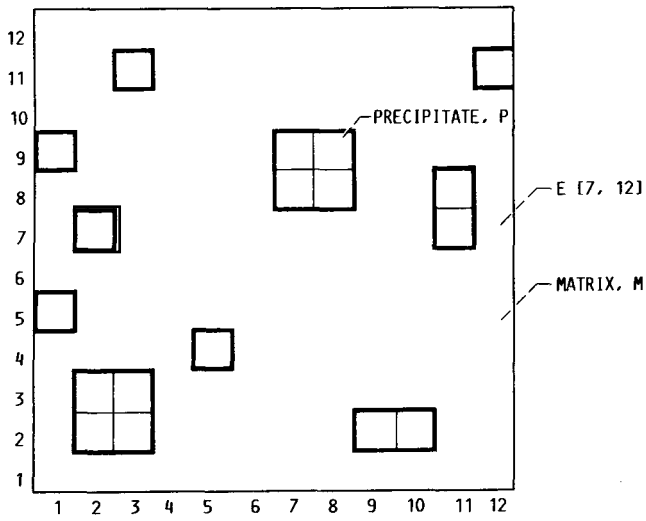


FIGURE 1. - GLOBAL NUMBERING SCHEME USED TO IDENTIFY INDIVIDUAL MONTE CARLO ELEMENTS. GRID TYPIFIES THAT OF A LOW VOLUME FRACTION, TWO PHASE MICROSTRUCTURE.

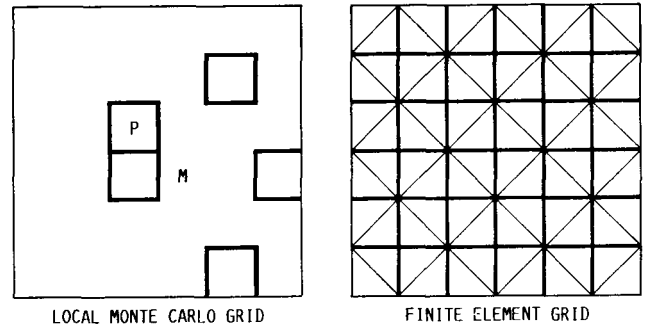


FIGURE 2. - LOCAL MONTE CARLO GRID GENERATED FROM GLOBAL GRID, FIGURE 1. NOTE CENTRAL LOCATION OF EXCHANGE PAIR P-M, E [7, 12] AND E [8, 11] OF GLOBAL GRID. ALSO SHOWN IS FINITE ELEMENT GRID COMPOSED OF 2D SIMPLEX TRIANGLES.

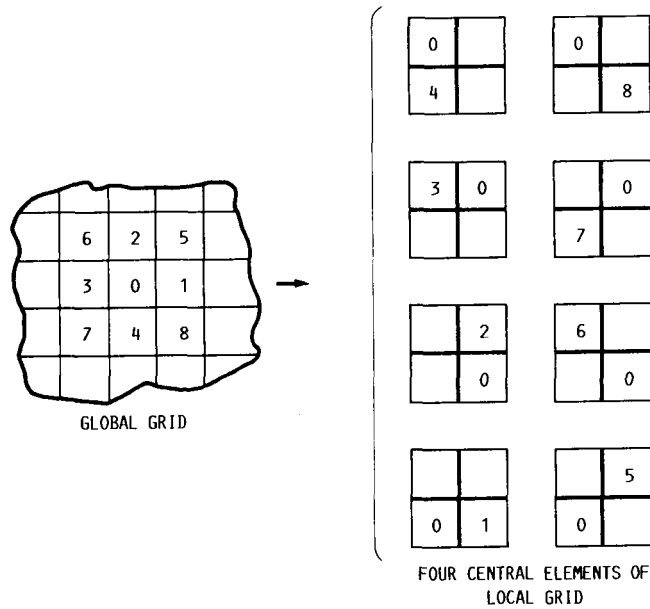
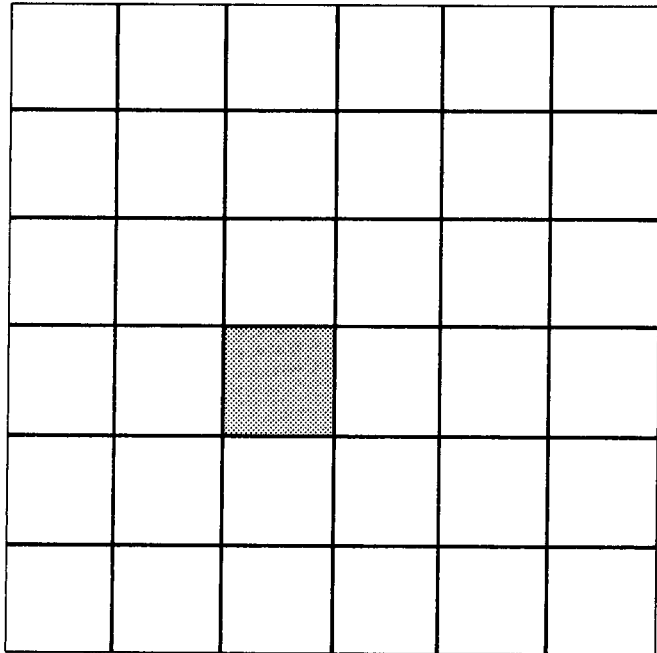


FIGURE 3. - LOGIC USED TO BUILD LOCAL MONTE CARLO GRID FROM GLOBAL GRID GIVEN SITE 0 AND AN EXCHANGE TYPE, 1 THRU 8.

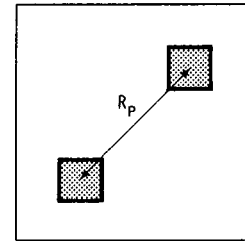


6x6 MONTE CARLO GRID

2	4	4	1	4	1
1	4	6	2	3	1
4	4	2	3	1	2
3	3	3	2	3	3
2	3	4	1	6	1
3	3	2	4	3	3

N/2

FIGURE 4. - RANDOM WALK EXPERIMENT FOR A SINGLE ELEMENT PARTICLE. THE NUMBER OF EXCHANGES, N, INVOLVING THE PRECIPITATE FOR EACH OF THE 36 LATTICE SITES APPEARS TO SHOW THERE IS NO POSITIONAL BIAS.



6x6 GRID

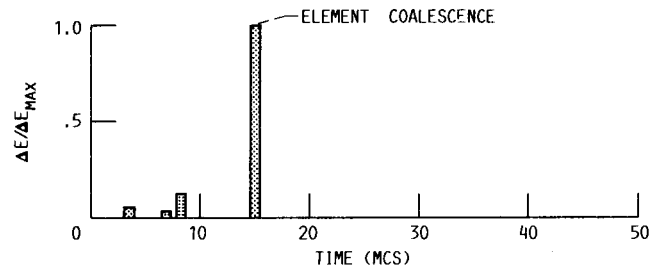
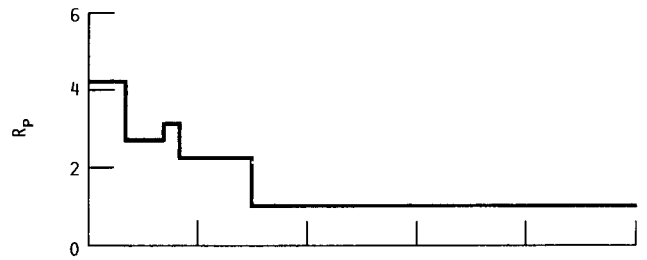
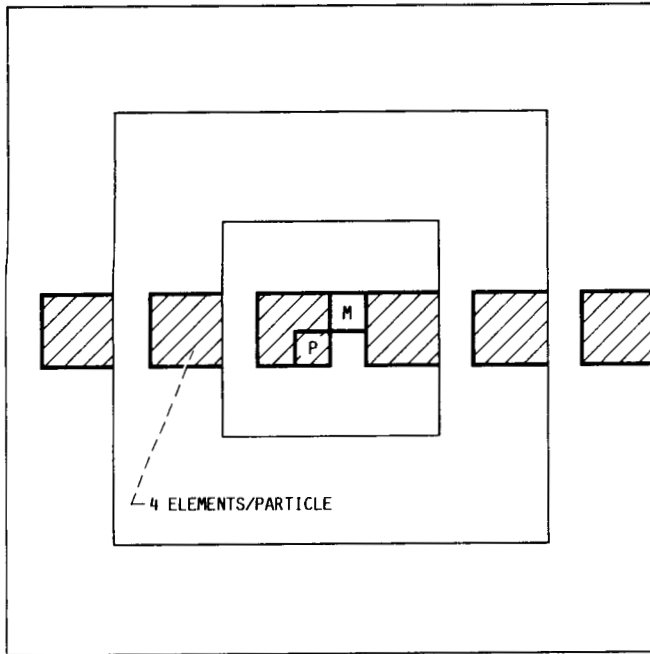


FIGURE 5. - ELEMENT INTERACTION ANALYSIS. NOTE THERE IS AN ATTRACTIVE FORCE BETWEEN THE TWO ELEMENTS. FURTHER, ELEMENT COALESCENCE PRODUCES THE GREATEST ENERGY CHANGE,  $\Delta E_{MAX}$ .



GRID SIZE (N)	$E_N'/E_{18}'$	$\Delta E_N'/\Delta E_{18}'$
6	0.132	0.992
12	0.464	0.981
18	1.000	1.000

FIGURE 6. - VARIATION OF INITIAL STRAIN ENERGIES,  $E_N'$ , AND CHANGE IN STRAIN ENERGIES,  $\Delta E_N'$ , ASSOCIATED WITH THE INTERCHANGE OF SITES P AND M AS A FUNCTION OF THE FINITE ELEMENT GRID SIZE, N.

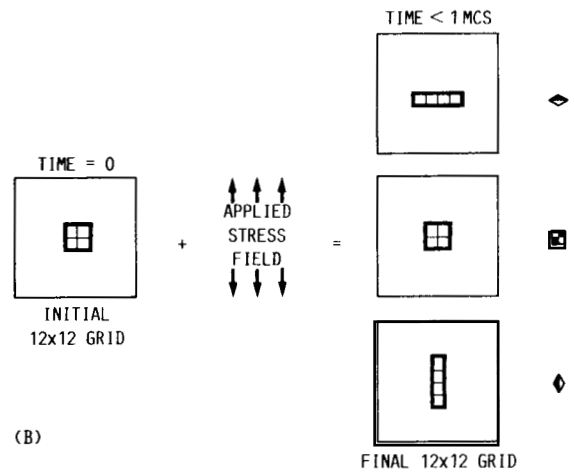
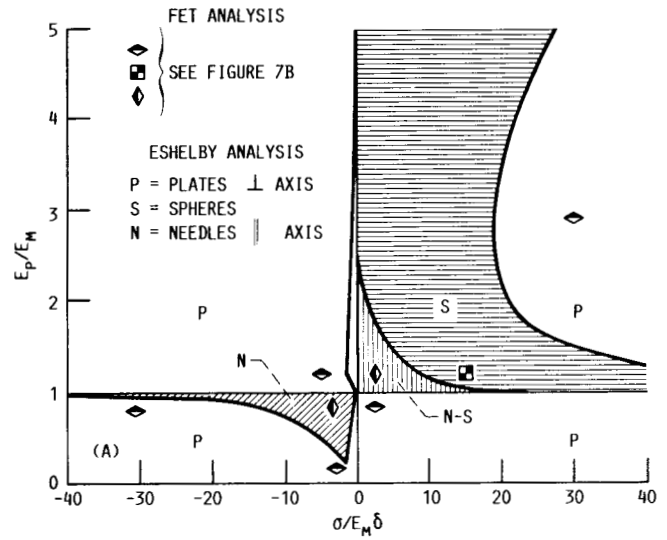


FIGURE 7. - COMPARISON OF FINITE ELEMENT ANALYSIS, FET, WITH PINEAU'S MAP, BASED ON ESHELBY ANALYSIS, FOR STRESS INDUCED SHAPE CHANGES OF A SINGLE PARTICLE, (A). SHAPE EVOLUTION OBSERVED IN MCFET SIMULATIONS OF SINGLE PARTICLE ANALYSIS, (B).

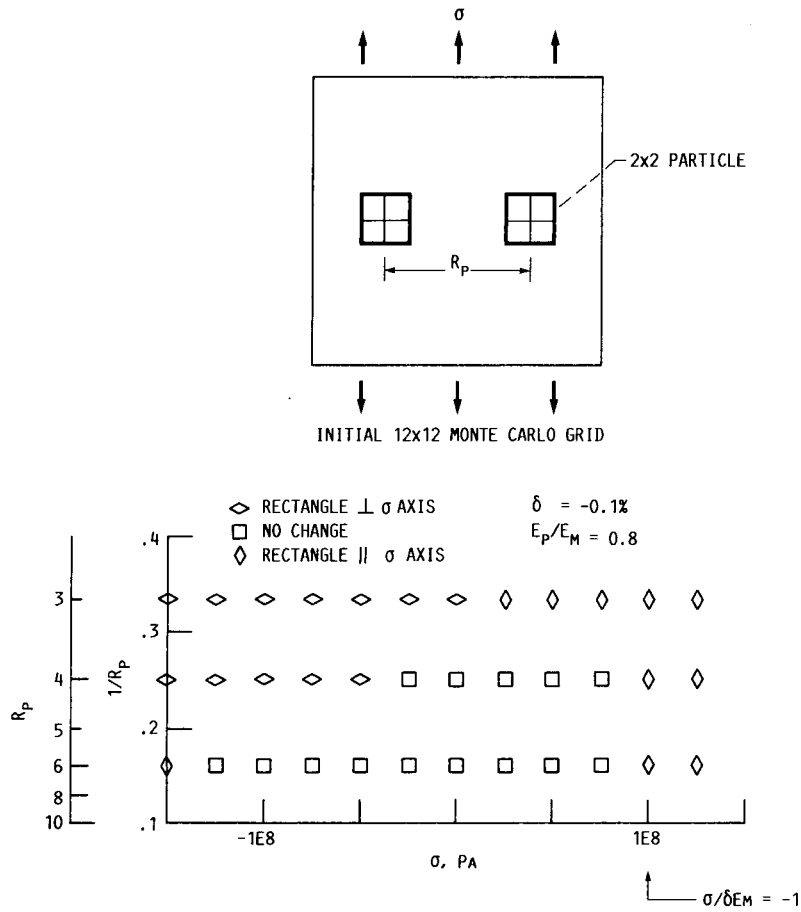


FIGURE 8. - EFFECT OF INTERPARTICLE SEPARATION,  $R_p$ , ON PARTICLE SHAPE AS A FUNCTION OF APPLIED STRESS,  $\sigma$ .

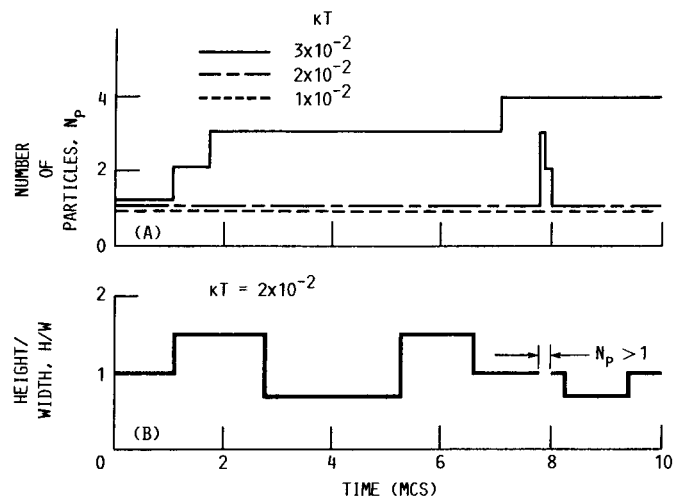


FIGURE 9. - SCALING OF THE THERMAL ENERGY TERM. (A) AS  $kT$  IS INCREASED THERE IS A GREATER TENDENCY FOR THE PARTICLE TO BREAK UP. (B) AT  $kT = 2 \times 10^{-2}$  THE PARTICLE SHAPE (H/W) CONTINUALLY CHANGES.

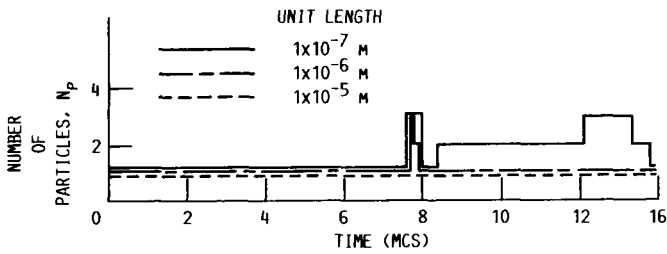


FIGURE 10. - CHANGING THE LENGTH UNIT DRAMATICALLY ALTERS THE IMPORTANCE OF SURFACE ENERGY BY CHANGING THE SURFACE AREA TO VOLUME RATIO. SMALLER PARTICLES (DECREASING UNIT LENGTH) HAVE MORE TENDANCE TO BREAK UP, I.E., THEY TEND TO DISSOLVE MORE READILY.

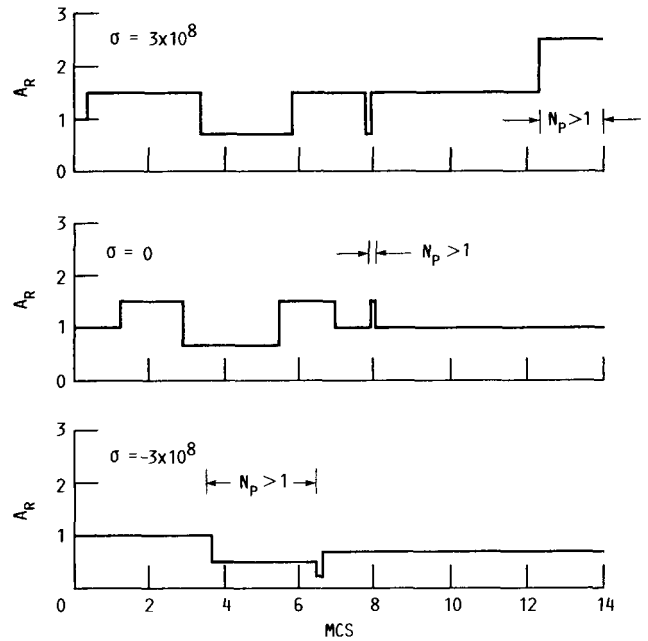


FIGURE 11. - EFFECT OF APPLIED STRESS ON PARTICLE ASPECT RATIO,  $A_R$ . WHEN  $N_p = 1$  THE ASPECT RATIO IS THE HEIGHT TO WIDTH RATIO OF THE SINGLE PARTICLE. WHEN  $N_p > 1$ , THE ASPECT RATIO IS AN AVERAGED HEIGHT TO WIDTH RATIO OF ALL PARTICLES. IN THIS ANALYSIS, AN H/W RATIO GREATER THAN 1 CORRESPONDS TO PARTICLE ELONGATION PARALLEL TO THE APPLIED STRESS AXIS.

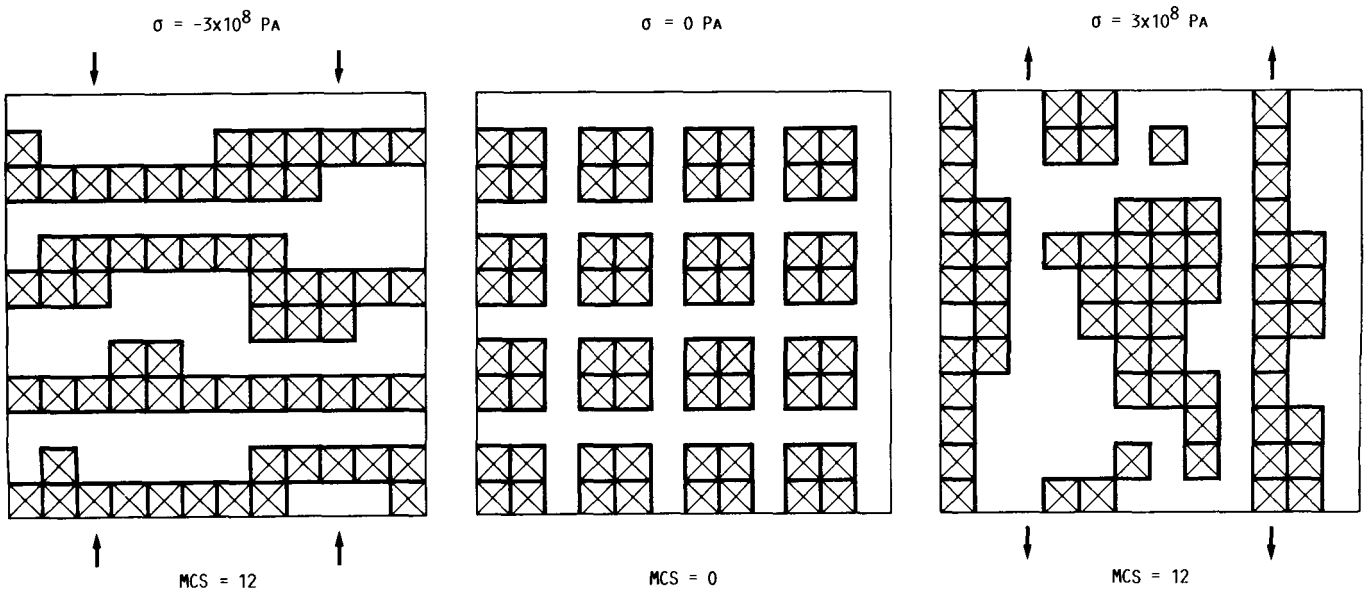


FIGURE 12. - EFFECT OF APPLIED STRESS ON A MULTI-PARTICLE MICROSTRUCTURE.



National Aeronautics and  
Space Administration

## Report Documentation Page

1. Report No. NASA TM-100215		2. Government Accession No.		3. Recipient's Catalog No.	
4. Title and Subtitle A Microstructural Lattice Model For Strain Oriented Problems: A Combined Monte Carlo Finite Element Technique				5. Report Date November 1987	
				6. Performing Organization Code	
7. Author(s) J. Gayda and D.J. Srolovitz				8. Performing Organization Report No. E-3824	
				10. Work Unit No. 505-63-11	
9. Performing Organization Name and Address National Aeronautics and Space Administration Lewis Research Center Cleveland, Ohio 44135-3191				11. Contract or Grant No.	
				13. Type of Report and Period Covered Technical Memorandum	
12. Sponsoring Agency Name and Address National Aeronautics and Space Administration Washington, D.C. 20546-0001				14. Sponsoring Agency Code	
15. Supplementary Notes J. Gayda, NASA Lewis Research Center; D.J. Srolovitz, University of Michigan, Ann Arbor, Michigan 48109.					
16. Abstract A specialized, microstructural lattice model, termed MCFET for combined Monte Carlo Finite Element Technique, has been developed which simulates microstructural evolution in material systems where modulated phases occur and the directionality of the modulation is influenced by internal and external stresses. In this approach the microstructure is discretized onto a fine lattice. Each element in the lattice is labelled in accordance with its microstructural identity. Diffusion of material at elevated temperatures is simulated by allowing exchanges of neighboring elements if the exchange lowers the total energy of the system. A Monte Carlo approach is used to select the exchange site while the change in energy associated with stress fields is computed using a finite element technique. The MCFET analysis has been validated by comparing this approach with a closed-form, analytical method for stress-assisted, shape changes of a single particle in an infinite matrix. Sample MCFET analytical for multiparticle problems have also been run and in general the resulting microstructural changes associated with the application of an external stress are similar to that observed in Ni-Al-Cr alloys at elevated temperatures.					
17. Key Words (Suggested by Author(s)) Modulated phases; Monte Carlo analysis; Finite element technique; Lattice models			18. Distribution Statement Unclassified - Unlimited Subject Category 26		
19. Security Classif. (of this report) Unclassified		20. Security Classif. (of this page) Unclassified		21. No of pages 29	22. Price* A03